[6] W. S. Cleveland, "Robust locally weighted regression and smoothing scatterplots," *J. Amer. Stat. Assoc.*, vol. 74, pp. 829–836, 1979.

[7] S. A. Cruces-Alvarez, A. Cichocki, and S. Amari, "From blind signal extraction to blind instantaneous signal separation: Criteria, algorithms, and stability," *IEEE Trans. Neural Netw.*, vol. 15, no. 4, pp. 859–873, Jul. 2004.

[8] W. De Clercq, A. Vergult, B. Vanrumste, W. Van Paesschen, and S. Van Huffel, "Canonical correlation analysis applied to remove muscle artifacts from the electroencephalogram," *IEEE Trans. Biomed. Eng.*, vol. 53, no. 12, pp. 2583–2587, Dec. 2006.

[9] B. De Moor, Daisy: Database for the Identification of Systems. [Online]. Available: http://www.esat.kuleuven.ac.be/sista/daisy

[10] D. H. Foley, "Considerations of sample and feature size," *IEEE Trans. Inf. Theory*, vol. IT-18, no. 5, pp. 618–626, Sep. 1972.

[11] O. Friman, M. Borga, P. Lundberg, and H. Knutsson, "Exploratory fMRI analysis by autocorrelation maximization," *NeuroImage*, vol. 16, no. 2, pp. 454–464, 2002.

[12] A. Green, M. Berman, P. Switzer, and M. Craig, "A transformation for ordering multispectral data in terms of image quality with implications for noise removal," *IEEE Trans. Geosci. Remote Sens.*, vol. 26, no. 1, pp. 65–74, Jan. 1988.

[13] D. R. Hundley, M. J. Kirby, and M. Anderle, "Blind source separation using the maximum signal fraction approach," *Signal Process.*, vol. 82, pp. 1505–1508, 2002.

[14] A. Hyvärinen, J. Karhunen, and E. Oja, *Independent Component Analysis*. New York: Wiley, 2001.

[15] A. Hyvärinen, "Fast and robust fixed-point algorithms for independent component analysis," *IEEE Trans. Neural Netw.*, vol. 10, no. 3, pp. 626–634, May 1999.

[16] "EEG Pattern Analysis," Comp. Sci. Dept., Colorado State Univ., Ft. Collins, CO [Online]. Available: http://www.cs.colostate.edu/eeg

[17] Y. Koren and L. Carmel, "Robust linear dimensionality reduction," *IEEE Trans. Vis. Comput. Graph.*, vol. 10, no. 4, pp. 459–470, Jul./Aug. 2004.

[18] T.-W. Lee, M. Girolami, and T. Sejnowski, "Independent component analysis using an extended infomax algorithm for mixed sub-Gaussian and super-Gaussian sources," *Neural Comput.*, vol. 11, no. 2, pp. 417–441, 1999.

[19] W. Liu, D. P. Mandic, and A. Cichocki, "Analysis and online realization of the CCA approach for blind source separation," *IEEE Trans. Neural Netw.*, vol. 18, no. 5, pp. 1505–1510, Sep. 2007.

[20] K.-R. Müller, C. W. Anderson, and G. E. Birch, "Linear and nonlinear methods for brain-computer interfaces," *IEEE Trans. Neural Syst. Rehabil. Eng.*, vol. 11, no. 2, pp. 165–169, Jun. 2003.

[21] H. Nam, T.-G. Yim, S. Han, J.-B. Oh, and S. Lee, "Independent component analysis of ictal EEG in medial temporal lobe epilepsy," *Epilepsia*, vol. 43, no. 2, pp. 160–164, 2002.

[22] E. Urrestarazu, J. Iriarte, M. Alegre, M. Valencia, C. Viteri, and J. Artieda, "Independent component analysis removing artifacts in ictal recordings," *Epilepsia*, vol. 45, no. 9, pp. 1071–1078, 2004.

[23] H. Wang and W. Zheng, "Local temporal common spatial patterns for robust single-trial EEG classification," *IEEE Trans. Neural Syst. Rehabil. Eng.*, vol. 16, no. 2, pp. 131–139, Apr. 2008.

[24] S. Yan, D. Xu, B. Zhang, H.-J. Zhang, Q. Yang, and S. Lin, "Graph embedding and extensions: A general framework for dimensionality reduction," *IEEE Trans. Pattern Anal. Mach. Intell.*, vol. 29, no. 1, pp. 40–51, Jan. 2007.

A Study of the LCMV and MVDR Noise Reduction Filters

Mehrez Souden, Jacob Benesty, and Sofiène Affes

Abstract—In real-world environments, the signals captured by a set of microphones in a speech communication system are mixtures of the desired signal, interference, and ambient noise. A promising solution for proper speech acquisition (with reduced noise and interference) in this context consists in using the linearly constrained minimum variance (LCMV) beamformer to reject the interference, reduce the overall mixture energy, and preserve the target signal. The minimum variance distortionless response beamformer (MVDR) is also commonly known to reduce the interference-plus-noise energy without distorting the desired signal. In either case, it is of paramount importance to accurately quantify the achieved noise and interference reduction. Indeed, it is quite reasonable to ask, for instance, about the price that has to be paid in order to achieve total removal of the interference without distorting the target signal when using the LCMV. Besides, it is fundamental to understand the effect of the MVDR on both noise and interference. In this correspondence, we investigate the performance of the MVDR and LCMV beamformers when the interference and ambient noise coexist with the target source. We demonstrate a new relationship between both filters in which the MVDR is decomposed into the LCMV and a matched filter (MVDR solution in the absence of interference). Both components are properly weighted to achieve maximum interference-plus-noise reduction. We investigate the performance of the MVDR, LCMV, and matched filters and elaborate new closed-form expressions for their output signal-to-interference ratio (SIR) and output signal-to-noise ratio (SNR). We theoretically demonstrate the tradeoff that has to be made between noise reduction and interference rejection. In fact, the total removal of the interference may severely amplify the residual ambient noise. Conversely, totally focussing on noise reduction leads to increased level of residual interference. The proposed study is finally supported by several numerical examples.

Index Terms—Beamforming, interference rejection, linearly constrained minimum variance (LCMV), minimum variance distortionless response (MVDR), noise reduction, speech enhancement.

I. INTRODUCTION

The omnipresence of acoustic noise and its profound effect on speech quality and intelligibility account for the great need to develop viable noise reduction techniques. To this end, a classical trend in noise reduction literature has been to split the microphone outputs into a target source and an additive component termed as noise that contains all other undesired signals. Then, the noise is reduced while the amount of target signal distortion is controlled [1]–[5]. In many practical scenarios, *both* interference, which is spatially correlated, and ambient noise components (e.g., spatially white and/or diffuse) *coexist* with the target source as in teleconferencing rooms and hearing aids applications, for example [2], [6]–[9]. This correspondence is concerned with noise reduction when the desired speech is contaminated with both interference and ambient noise.

The spatio-temporal processing of signals is widely known as "beamforming" and it has been delineated in several ways to extract

a target from a mixture of signals captured by a set of sensors. Early beamforming techniques were developed under the assumption that the channel effect can be modeled by a delay and attenuation only. In actual room acoustics, however, the propagation process is much more complex [10], [11]. Indeed, the propagating signals undergo several reflections before impinging on the microphones. To address this issue, Frost proposed a general framework for adaptive time-domain implementation of the MVDR, originally proposed by Capon [12], in which a finite-duration impulse response (FIR) filter is applied to each microphone output. These filtered signals are then summed together to reinforce the target signal and reduce the background noise [13]. In [1], Kaneda and Ohga considered the generalized channel transfer functions (TFs) and proposed an adaptive algorithm that achieves a tradeoff between noise reduction and signal distortion. In [14], Affes and Grenier proposed an adaptive channel TF-based generalized sidelobe canceler (GSC), an alternative implementation of the MVDR [15], that tracks the signal subspace to jointly reduce the noise and the reverberation. In [3], Gannot *et al.* considered noise reduction using the GSC and showed that it depends on the channel TF ratios since the objective was to reconstruct a reference noise-free and reverberant speech signal. In [16], Markovich *et al.* proposed an LCMV-based approach for speech enhancement in reverberant and noisy environments.

Besides the great efforts to develop reliable noise reduction techniques, many contributions have been made to understand their functioning and accurately quantify their gains and losses in terms of speech distortion and noise reduction. In [17], Bitzer *et al.* investigated the theoretical performance limits of the GSC beamformer in the case of a spatially diffuse noise. In [18], the theoretical equivalence between the LCMV and its GSC counterpart was demonstrated. In [5], theoretical expressions showing the tradeoff between noise reduction and speech distortion in the parameterized multichannel Wiener filtering were established. In [19], Gannot and Cohen studied the noise reduction ability of the channel TF ratio-based GSC beamformer. They found that it is theoretically possible to achieve infinite noise reduction when only a spatially coherent noise is added to the speech. Actually, the total removal of the interference while preserving the target signal reminds us of the the LCMV beamformer which passes the desired signal through and rejects the interference.

Here, we assume that *both* interference and ambient noise *coexist* with the target source. This assumption is quite plausible when hands-free full duplex communication devices are deployed within a teleconferencing room, for instance [4], [16]. In this situation, the target signal is generated by one speaker while the interference is more likely to be generated by another participant or a device (e.g., fan or computer) located within the same room. In addition, ambient noise is ubiquitous in these environments and it is quite reasonable to take it into consideration. A clear understanding of the functioning of noise reduction algorithms in terms of both interference and other noise reduction capabilities in this case is crucial. In this contribution, we are interested in reducing the noise and interference without distorting the target signal. A potential solution to this problem consists in nulling the interference, preserving the target source, and minimizing the overall energy. This doubly constrained formulation is termed LCMV beamformer in the sequel. The MVDR is also a good alternative to perform this task.

Notable efforts to analyze the MVDR performance in the presence of additive noise and interferences include [9] where Wax and Anu investigated its output SINR when the additive noise is *spatially white* with identically distributed (i.d.) components. In [8], the array gain and beampattern of the MVDR were studied under the assumptions of *plane-wave* propagation model and *spatially white* additive noise with i.d. components. This scenario is more appropriate for radar and wireless communication systems where the scattering is negligible [8].

Herein, we study the tradeoff between noise reduction and interference rejection for speech acquisition using the MVDR and LCMV in acoustic rooms where the channel effect is modeled by *generalized TFs*. Also, we consider the general case of *arbitrary* additive noise (referred to as ambient noise here). Fundamental results are demonstrated to clearly highlight this tradeoff. Indeed, we first prove that the MVDR is composed of the LCMV and a matched filter (MVDR solution in the absence of interference); both components are properly weighted to achieve maximum interference-plus-noise reduction. For generality, we further propose a new parameterized beamformer which is composed of the LCMV and matched filters. This new beamformer has the MVDR, LCMV, and matched filters as particular cases. Afterwards, we provide a generalized analysis that shows the effect of this parameterized beamformer on both output SIR and output SNR and theoretically establish the tradeoff of interference rejection versus ambient noise reduction with a special focus on the MVDR, LCMV, and matched filters.

This correspondence is organized as follows. Section II describes the signal propagation model, definitions, and assumptions. Section III outlines the formulations leading to the MVDR and LCMV and the new relationship between both beamformers. Section IV investigates the performance of the parameterized noise reduction beamformer with a special focus on the MVDR, LCMV, and matched filters. Section V corroborates the analytical analysis through several numerical examples. Section VI contains some concluding remarks.

II. PRELIMINARIES: SIGNAL PROPAGATION MODEL AND DEFINITIONS

A. Data Model

Let $s[t]$ denote a target speech signal impinging on an array of M microphones with an arbitrary geometry in addition to an interfering source $\psi[t]$ and some unknown additive noise at a discrete time instant t. The resulting observations are given by

$$y_n[t] = x_n[t] + i_n[t] + v_n[t] \tag{1}$$

where $x_n[t] = g_n * s[t]$, $i_n[t] = d_n * \psi[t]$, $*$ is the convolution operator, $g_n[t]$ and $d_n[t]$ are the channel impulse responses encountered by the target and interfering sources, respectively, before impinging on the nth microphone, and $v_n[t]$ is the unknown ambient noise component at microphone n (this model remains valid when multiple interferers are present since we can focus on the effect of a single interferer and group all other undesired signals in the noise term). $\psi[t]$ and $s[t]$ are mutually uncorrelated. The noise components are also uncorrelated with $\psi[t]$ and $s[t]$. Moreover, all signals are assumed to be zero-mean random processes. The above data model can be written in the frequency domain as

$$Y_n(j\omega) = X_n(j\omega) + I_n(j\omega) + V_n(j\omega), \quad n = 1, 2, \ldots, M, \tag{2}$$

where $Y_n(j\omega)$, $X_n(j\omega) = G_n(j\omega)S(j\omega)$, $I_n(j\omega) = D_n(j\omega)\Psi(j\omega)$, $G_n(j\omega)$, $S(j\omega)$, $D_n(j\omega)$, $\Psi(j\omega)$, and $V_n(j\omega)$ are the discrete time Fourier transforms (DTFTs) of $y_n[t]$, $x_n[t]$, $i_n[t]$, $g_n[t]$, $s[t]$, $d_n[t]$, $\psi[t]$ and $v_n[t]$, respectively.[1] The remainder of our study is frequency-bin-wise and we will avoid explicitly mentioning the dependence of all the involved terms on ω in the sequel for conciseness.

Our aim is to reduce the noise and recover one of the noise-free speech components, say X_1, the best way we can (along some criteria to be defined later) by applying a linear filter $\mathbf{h}$ to the observations'

---

[1]We do not take into account the windowing effect that happens in practice for heavily reverberant environments with short frames when using the short time Fourier transform instead of the DTFT.

vector $\mathbf{y} = [Y_1 \, Y_2 \, \cdots \, Y_M]^T$ where $(\cdot)^T$ denotes the transpose operator. The output of $\mathbf{h}$ is given by

$$Z = \mathbf{h}^H \mathbf{y} = \mathbf{h}^H \mathbf{x} + \mathbf{h}^H \mathbf{i} + \mathbf{h}^H \mathbf{v} \quad (3)$$

where $\mathbf{x}$, $\mathbf{i}$, and $\mathbf{v}$ are defined in a similar way to $\mathbf{y}$, $\mathbf{h}^H \mathbf{x}$ is the output speech component, $\mathbf{h}^H \mathbf{i}$ is the residual interference, $\mathbf{h}^H \mathbf{v}$ is the residual noise, and $(\cdot)^H$ denotes transpose-conjugate operator.

Definitions

We first define the two vectors containing all the channel transfer functions between the source, interference, and microphones' locations as $\mathbf{g} = [G_1, G_2, \ldots, G_M]^T$ and $\mathbf{d} = [D_1, D_2, \ldots, D_M]^T$. Also, we define the power spectrum density (PSD) matrix for a given vector $\mathbf{a}$ as $\mathbf{\Phi}_{aa} = E\left\{\mathbf{a}\mathbf{a}^H\right\}$.

Since we are taking the first noise-free microphone signal as a reference, we define the local (frequency bin-wise) input SNR as $\mathrm{SNR} = \phi_{x_1 x_1}/\phi_{v_1 v_1}$, where $\phi_{aa} = E\left\{|A|^2\right\}$ is the PSD of $a[t]$ (having A as DTFT). We also define the local input SIR as $\mathrm{SIR} = \phi_{x_1 x_1}/\phi_{i_1 i_1}$, the local input signal-to-interference-plus-noise ratio (SINR) as $\mathrm{SINR} = \phi_{x_1 x_1}/\phi_{i_1 i_1} + \phi_{v_1 v_1}$ and the local input interference-to-noise ratio (INR) which is given by $\mathrm{INR} = \phi_{i_1 i_1}/\phi_{v_1 v_1}$. The SNR, SIR, and SINR at the output of a given filter $\mathbf{h}$ are, respectively, defined as $\mathrm{SNR}_o(\mathbf{h}) = \mathbf{h}^H \mathbf{\Phi}_{xx} \mathbf{h}/\mathbf{h}^H \mathbf{\Phi}_{vv} \mathbf{h}$, $\mathrm{SIR}_o(\mathbf{h}) = \mathbf{h}^H \mathbf{\Phi}_{xx} \mathbf{h}/\mathbf{h}^H \mathbf{\Phi}_{ii} \mathbf{h}$, and $\mathrm{SINR}_o(\mathbf{h}) = \mathbf{h}^H \mathbf{\Phi}_{xx} \mathbf{h}/\mathbf{h}^H \mathbf{\Phi}_{ii} \mathbf{h} + \mathbf{h}^H \mathbf{\Phi}_{vv} \mathbf{h}$. In order to obtain an optimal estimate of X_1 at every frequency bin at the output of $\mathbf{h}$, we define the error signals $\mathcal{E}_x = (\mathbf{u}_1 - \mathbf{h})^H \mathbf{x}$, $\mathcal{E}_i = \mathbf{h}^H \mathbf{i}$, and $\mathcal{E}_v = \mathbf{h}^H \mathbf{v}$, where $\mathbf{u}_1 = [1 \, 0 \, \cdots \, 0]^T$ is an M-dimensional vector. $\mathcal{E}_x$, $\mathcal{E}_i$, and $\mathcal{E}_v$ are the residual signal distortion, interference, and noise at the output of $\mathbf{h}$, respectively.

In this correspondence, we investigate two noise reduction filters: the MVDR which aims at reducing the interference-plus-noise without distorting the target signal and the LCMV which totally eliminates the interference and preserves the desired signal. Next, we formulate both objectives mathematically, demonstrate a simplified relationship between both filters, and rigorously analyze their performance.

III. GENERAL FORMULATION OF THE MVDR AND LCMV BEAMFORMERS

The formulations of the LCMV and MVDR filters investigated here share the common objectives of attempting to reduce the noise and interference while preserving the target signal. In order to meet the second objective, we impose the constraint $\mathcal{E}_x = (\mathbf{u}_1 - \mathbf{h})^H \mathbf{g} S = 0$ or equivalently (assuming $S \neq 0$)

$$\mathbf{h}^H \mathbf{g} = G_1. \quad (4)$$

In the sequel, this constraint will be taken into consideration in the formulation of the noise reduction filters. Also, it is important to point out, before proceeding, the following property.

1) Property 1: The matrices $\mathbf{\Phi}_{vv}^{-1} \mathbf{\Phi}_{xx}$ and $\mathbf{\Phi}_{vv}^{-1} \mathbf{\Phi}_{ii}$ are each of rank 1. The two strictly positive eigenvalues of both matrices are denoted as $\gamma_{x,v}$ and $\gamma_{i,v}$ and expressed as

$$\gamma_{x,v} = \mathrm{tr}\left[\mathbf{\Phi}_{vv}^{-1} \mathbf{\Phi}_{xx}\right] \quad (5)$$

$$\gamma_{i,v} = \mathrm{tr}\left[\mathbf{\Phi}_{vv}^{-1} \mathbf{\Phi}_{ii}\right] \quad (6)$$

respectively, where $\mathrm{tr}[\cdot]$ denotes the trace of a square matrix. We also have the two following factorizations

$$\mathbf{\Phi}_{vv}^{-1} \mathbf{\Phi}_{xx} = \gamma_{x,v} \mathbf{c}_x \mathbf{l}_x^T \quad (7)$$

$$\mathbf{\Phi}_{vv}^{-1} \mathbf{\Phi}_{ii} = \gamma_{i,v} \mathbf{c}_i \mathbf{l}_i^T \quad (8)$$

where $\mathbf{c}_x$ and $\mathbf{l}_x^T$ are the first column and first line of the matrices $\mathbf{P}$ and $\mathbf{P}^{-1}$, respectively. $\mathbf{P}$ is the matrix that diagonalizes $\mathbf{\Phi}_{vv}^{-1} \mathbf{\Phi}_{xx}$, i.e., $\mathbf{\Phi}_{vv}^{-1} \mathbf{\Phi}_{xx} = \mathbf{P} \mathbf{\Gamma}_x \mathbf{P}^{-1}$ and $\mathbf{\Gamma}_x = \mathrm{diag}\left[\gamma_{x,v}, 0, \ldots, 0\right]$. Similarly, we define $\mathbf{c}_i$ and $\mathbf{l}_i^T$ as the first column and first line of the matrices $\mathbf{Q}$ and $\mathbf{Q}^{-1}$, respectively, where $\mathbf{Q}$ satisfies $\mathbf{\Phi}_{vv}^{-1} \mathbf{\Phi}_{ii} = \mathbf{Q} \mathbf{\Gamma}_i \mathbf{Q}^{-1}$ and $\mathbf{\Gamma}_i = \mathrm{diag}\left[\gamma_{i,v}, 0, \ldots, 0\right]$. $\qquad\square$

We further define the collinearity factor

$$\kappa = \left(\mathbf{l}_i^T \mathbf{c}_x\right)\left(\mathbf{l}_x^T \mathbf{c}_i\right). \quad (9)$$

Using the Cauchy–Schwarz inequality, it is easy to prove that $0 \leq \kappa \leq 1$. Indeed,

$$\begin{aligned} \kappa &= \mathrm{tr}\left[\mathbf{c}_i \mathbf{l}_i^T \mathbf{c}_x \mathbf{l}_x^T\right] \\ &= \frac{\mathrm{tr}\left[\mathbf{\Phi}_{vv}^{-1} \mathbf{\Phi}_{ii} \mathbf{\Phi}_{vv}^{-1} \mathbf{\Phi}_{xx}\right]}{\gamma_{x,v} \gamma_{i,v}} \\ &= \frac{\left|\mathbf{g}^H \mathbf{\Phi}_{vv}^{-1} \mathbf{d}\right|^2}{\mathbf{g}^H \mathbf{\Phi}_{vv}^{-1} \mathbf{g} \mathbf{d}^H \mathbf{\Phi}_{vv}^{-1} \mathbf{d}}. \end{aligned}$$

To interpret the physical meaning of κ, let us use this eigendecomposition $\mathbf{\Phi}_{vv}^{-1} = \mathbf{V} \mathbf{\Lambda} \mathbf{V}^H$, where $\mathbf{V}$ is a unitary matrix since $\mathbf{\Phi}_{vv}^{-1}$ is Hermitian, and $\mathbf{\Lambda}$ contains all the eigenvalues of $\mathbf{\Phi}_{vv}^{-1}$. $\mathbf{\Phi}_{vv}^{-1}$ can also be decomposed as $\mathbf{\Phi}_{vv}^{-1} = \mathbf{\Phi}_{vv}^{-1/2} \mathbf{\Phi}_{vv}^{-1/2}$ where $\mathbf{\Phi}_{vv}^{-1/2} = \mathbf{V} \mathbf{\Lambda}^{1/2} \mathbf{V}^H$. Let us also define $\mathbf{a}_x = \mathbf{\Phi}_{vv}^{-1/2} \mathbf{g}$ and $\mathbf{a}_i = \mathbf{\Phi}_{vv}^{-1/2} \mathbf{d}$. Then, we deduce that

$$\kappa = \frac{\left|\mathbf{a}_x^H \mathbf{a}_i\right|^2}{\|\mathbf{a}_x\|^2 \|\mathbf{a}_i\|^2}. \quad (10)$$

Therefore, the larger is κ, the more collinear are $\mathbf{a}_x$ and $\mathbf{a}_i$ which are nothing but the propagation vectors of desired signal and the interference, respectively, up to the linear transformation $\mathbf{\Phi}_{vv}^{-1/2}$ which is traditionally known to standardize (whitening and normalization) [20] noise components. The definition of κ generalizes the so-called *spatial correlation factor* in [8], [9] to the investigated data model where the additive ambient noise has an arbitrary PSD matrix $\mathbf{\Phi}_{vv}$ and the channel effect is modeled by arbitrary transfer functions. Such assumptions are more realistic and apply to acoustic environments.

Finally, we define another important term that will be needed in the following analysis

$$\begin{aligned} \gamma &= \mathrm{tr}\left[\mathbf{\Phi}_{vv}^{-1} \mathbf{\Phi}_{ii}\right] \mathrm{tr}\left[\mathbf{\Phi}_{vv}^{-1} \mathbf{\Phi}_{xx}\right] - \mathrm{tr}\left[\mathbf{\Phi}_{vv}^{-1} \mathbf{\Phi}_{ii} \mathbf{\Phi}_{vv}^{-1} \mathbf{\Phi}_{xx}\right] \\ &= \gamma_{i,v} \gamma_{x,v} (1 - \kappa). \end{aligned} \quad (11)$$

A. Minimum Variance Distortionless Response Beamformer

In the general formulation of the MVDR for noise reduction, the recovery of the noise-free signal consists in minimizing the overall interference-plus-noise power subject to no speech distortion constraint. Then, the MVDR beamformer is mathematically obtained by solving the following optimization problem [3]–[5], [7]:

$$\mathbf{h}_{\mathrm{MVDR}} = \arg\min_{\mathbf{h}} E\left\{|\mathcal{E}_v + \mathcal{E}_i|^2\right\} = \mathbf{h}^H \left(\mathbf{\Phi}_{ii} + \mathbf{\Phi}_{vv}\right) \mathbf{h}$$
$$\text{subject to} \quad \mathbf{g}^H \mathbf{h} = G_1^*. \quad (12)$$

The solution to this optimization problem is given by [3], [7]

$$\mathbf{h}_{\mathrm{MVDR}} = G_1^* \frac{\left(\mathbf{\Phi}_{ii} + \mathbf{\Phi}_{vv}\right)^{-1} \mathbf{g}}{\mathbf{g}^H \left(\mathbf{\Phi}_{ii} + \mathbf{\Phi}_{vv}\right)^{-1} \mathbf{g}}. \quad (13)$$

In [3], [4], and [19], the channel transfer function ratios were used to implement the GSC version of the above filter. By taking advantage of the fact that for a given matrix $\mathbf{M}$, we have $\mathbf{g}^H \mathbf{M} \mathbf{g} = \mathrm{tr}[\mathbf{M} \mathbf{\Phi}_{xx}]/\phi_{ss}$,

a more simplified form that relies on the overall noise and target signal PSD matrices was proposed in [5], [7] and is given by

$$\mathbf{h}_{\mathrm{MVDR}} = \frac{\left(\boldsymbol{\Phi}_{ii} + \boldsymbol{\Phi}_{vv}\right)^{-1}\boldsymbol{\Phi}_{xx}}{\operatorname{tr}\left[\left(\boldsymbol{\Phi}_{ii} + \boldsymbol{\Phi}_{vv}\right)^{-1}\boldsymbol{\Phi}_{xx}\right]}\mathbf{u}_1 \qquad (14)$$

in our case. When only the ambient noise $\mathbf{v}$ is superimposed to the desired signal [i.e., $\mathbf{i} = \mathbf{0}$], the MVDR solution reduces to

$$\mathbf{h}_{\mathrm{MATCH}} = \frac{\boldsymbol{\Phi}_{vv}^{-1}\boldsymbol{\Phi}_{xx}\mathbf{u}_1}{\gamma_{x,v}} \qquad (15)$$

where $\gamma_{x,v}$ is defined in (5). In the sequel, $\mathbf{h}_{\mathrm{MATCH}}$ is termed as matched filter.

B. Linearly Constrained Minimum Variance Beamformer

In the data model (1), the interference is modeled as a source that competes with the target signal. In order to remove it through spatial filtering, a common practice has been to zero the array response toward its direction of arrival. In the investigated scenario, we consider the general channel TFs between the location from which $\psi(t)$ is emitted and each of the microphone elements. Consequently, we force the constraint $\mathcal{E}_i = 0$ which is equivalent to

$$\mathbf{d}^H\mathbf{h} = 0. \qquad (16)$$

Since we are interested in obtaining a non-distorted version of the target signal, we also require the constraint (4) to be satisfied. Combining (4) and (16), we obtain $\mathbf{C}^H\mathbf{h} = G_1^*\tilde{\mathbf{u}}_1$, where $\mathbf{C} = [\mathbf{g}\ \mathbf{d}]$ and $\tilde{\mathbf{u}}_1 = [1\ 0]^T$. The ambient noise modeled by $\mathbf{v}$ has no specific structure. Therefore, the best that we can do to alleviate its effect is by reducing its power at the output of $\mathbf{h}$. Subsequently, we formulate the LCMV optimization problem that nulls the interference, reduces the noise, and preserves the speech [16]

$$\mathbf{h}_{\mathrm{LCMV}} = \arg\min_{\mathbf{h}} \mathbf{h}^H\boldsymbol{\Phi}_{vv}\mathbf{h}$$
$$\text{subject to} \quad \mathbf{C}^H\mathbf{h} = G_1^*\tilde{\mathbf{u}}_1. \qquad (17)$$

The solution to (17) is given by

$$\mathbf{h}_{\mathrm{LCMV}} = G_1^*\boldsymbol{\Phi}_{vv}^{-1}\mathbf{C}\left(\mathbf{C}^H\boldsymbol{\Phi}_{vv}^{-1}\mathbf{C}\right)^{-1}\tilde{\mathbf{u}}_1. \qquad (18)$$

In order to obtain (18), we assumed that $\left(\mathbf{C}^H\boldsymbol{\Phi}_{vv}^{-1}\mathbf{C}\right)$ is invertible, thereby implying that $M \geq 2$.

C. Relationship Between the MVDR and the LCMV Beamformers

In [4], [19], it was observed that when only spatially coherent noise (termed interference herein) overlaps to the desired source, the GSC (consequently its MVDR counterpart) is able to totally remove it. This fact does not seem to be straightforward to observe in the general expression of the MVDR since a fundamental requirement for this beamformer to exist is that the noise PSD matrix is invertible. To overcome this issue, Gannot and Cohen resorted to regularizing this matrix with a very small factor [19]. Then, it was observed that when this regularization factor is negligible, the MVDR steers a zero toward the interference. This behavior reminds us of the LCMV beamformer which passes the desired signal through and rejects the interference. Intuitively, a relationship between both beamformers seems to exist in general situations where both interference and ambient noise with full rank PSD matrix coexist. Herein, we confirm this intuition and establish a new simplified relationship between both filters.

Following the proof in Appendix I, we find the following decomposition of the MVDR:

$$\mathbf{h}_{\mathrm{MVDR}} = \rho_1\mathbf{h}_{\mathrm{LCMV}} + (1 - \rho_1)\mathbf{h}_{\mathrm{MATCH}} \qquad (19)$$

where

$$\rho_1 = \frac{\gamma}{\gamma + \gamma_{x,v}}. \qquad (20)$$

We easily see that

$$0 \leq \rho_1 \leq 1. \qquad (21)$$

The new relationship (19) between the MVDR, LCMV, and matched filters has a very attractive form in which we see that the MVDR attempts to both reducing the ambient noise by means of $\mathbf{h}_{\mathrm{MATCH}}$ and rejecting the interference by means of $\mathbf{h}_{\mathrm{LCMV}}$. The two components are properly weighted to prevent the target signal distortion and achieve a certain tradeoff between both objectives. To have better insights into the behavior of the MVDR, we consider the case where the ambient noise is white with identically distributed components in the following subsection.

D. Particular Case: Spatially White Noise

Here, we suppose that the PSD matrix of the ambient noise is given by $\boldsymbol{\Phi}_{vv} = \sigma^2\mathbf{I}$. From (19) and (20), we deduce that in order to study the behavior of the MVDR, we simply have to observe the variations of ρ_1. Subsequently, by replacing $\boldsymbol{\Phi}_{vv}$ by its expression in this particular case, we obtain

$$\rho_1 = \frac{\mathrm{INR}\left[\|\tilde{\mathbf{g}}\|^2\left\|\tilde{\mathbf{d}}\right\|^2 - \left|\tilde{\mathbf{g}}^H\tilde{\mathbf{d}}\right|^2\right]}{\mathrm{INR}\left[\|\tilde{\mathbf{g}}\|^2\left\|\tilde{\mathbf{d}}\right\|^2 - \left|\tilde{\mathbf{g}}^H\tilde{\mathbf{d}}\right|^2\right] + \|\tilde{\mathbf{g}}\|^2} \qquad (22)$$

where $\tilde{\mathbf{g}} = \mathbf{g}/G_1$, and $\tilde{\mathbf{d}} = \mathbf{d}/D_1$ (both are vectors of the channel transfer function ratios). It is interesting to see that ρ_1 depends on two terms. The first one is INR, while the second purely depends on the geometric (or spatial) information relating the transfer functions between the target source, the interference, and the microphones' locations $\|\tilde{\mathbf{g}}\|^2\left\|\tilde{\mathbf{d}}\right\|^2 - \left|\tilde{\mathbf{g}}^H\tilde{\mathbf{d}}\right|^2/\|\tilde{\mathbf{g}}\|^2$. Let us further use this decomposition $\tilde{\mathbf{d}} = \tilde{\mathbf{d}}_\perp + \tilde{\mathbf{d}}_\parallel$, where $\tilde{\mathbf{d}}_\parallel = \mu\tilde{\mathbf{g}}$ with $\mu = \tilde{\mathbf{g}}^H\tilde{\mathbf{d}}/\|\tilde{\mathbf{g}}\|^2$, and $\tilde{\mathbf{d}}_\perp = \tilde{\mathbf{d}} - \mu\tilde{\mathbf{g}}$ is orthogonal to $\mathbf{g}$. Then, we have

$$\rho_1 = \frac{1}{1 + r_\perp} \qquad (23)$$

where $r_\perp = \sigma^2/\phi_{i_1i_1}\left\|\tilde{\mathbf{d}}_\perp\right\|^2$. We infer from (23) that $\lim_{r_\perp \to +\infty}\rho_1 = 0$, thereby meaning that

$$\lim_{r_\perp \to +\infty}\mathbf{h}_{\mathrm{MVDR}} = \mathbf{h}_{\mathrm{MATCH}}. \qquad (24)$$

Also, $\lim_{r_\perp \to 0}\rho_1 = 1$, thereby meaning that

$$\lim_{r_\perp \to 0}\mathbf{h}_{\mathrm{MVDR}} = \mathbf{h}_{\mathrm{LCMV}}. \qquad (25)$$

Consequently, we conclude that when the energy of the coherent noise component which is *orthogonal* to $\tilde{\mathbf{g}}$ is much larger than the energy of the unknown noise, the MVDR filter behaves like the LCMV. Conversely, when this energy is low, the MVDR behaves like the matched filter.

IV. Generalized Distortionless Beamformer and Performance Analysis

Based on our analysis in Section III, we see that the matched filter aims at reducing the ambient noise and totally ignores the interference in its formulation. The LCMV corresponds to another extreme since it totally removes the interference, while the MVDR attempts to optimally reduce both interference and noise and achieves a certain tradeoff between the LCMV and the matched filter. In the following, we propose a parameterized beamformer whose expression is similar to the MVDR. Then, we evaluate its output noise reduction capabilities with a special focus on the MVDR, LCMV, and matched filters.

A. Generalized Distortionless Beamformer

Inspired by the new decomposition of the MVDR filter in (19) and (20), we propose a new parameterized beamformer for noise reduction that we define as

$$\mathbf{h}_{\mathrm{p}} = \rho \mathbf{h}_{\mathrm{LCMV}} + (1 - \rho) \mathbf{h}_{\mathrm{MATCH}} \qquad (26)$$

where ρ is a tuning parameter that satisfies the condition

$$0 \le \rho \le 1 \qquad (27)$$

in order to have a distortionless response. In fact, we can easily verify that under the above condition, we have $\mathbf{h}_{\mathrm{p}}^{H} \mathbf{g} = G_1$. For the sake of generality, we analyze the noise reduction capability of $\mathbf{h}_{\mathrm{p}}$ and deduce the effect of the tuning parameter ρ.

B. Performance Analysis

Since we are interested in filters that reduce the noise and interference without distorting the noise-free reference speech signal, we focus our attention on the study of the output SNR and output SIR. It is easy to see that the MVDR, LCMV, and matched filters are particular cases of the proposed parameterized beamformer, $\mathbf{h}_{\mathrm{p}}$. Consequently, for the sake of generality, we analyze the performance of the latter and show the effect of its tuning parameter ρ on both performance measures.

Following the proof given in Appendix II, we have

$$\mathbf{h}_{\mathrm{p}}^{H} \mathbf{\Phi}_{vv} \mathbf{h}_{\mathrm{p}} = \frac{\phi_{x_1 x_1}}{\gamma_{x,v}} \cdot \frac{1 - (1 - \rho^2) \kappa}{1 - \kappa}. \qquad (28)$$

The corresponding output SNR is

$$\mathrm{SNR_o}(\mathbf{h}_{\mathrm{p}}) = \gamma_{x,v} \frac{1 - \kappa}{1 - (1 - \rho^2) \kappa}. \qquad (29)$$

Also, we quantify the residual interference at the output of $\mathbf{h}_{\mathrm{p}}$ as shown in Appendix II

$$\mathbf{h}_{\mathrm{p}}^{H} \mathbf{\Phi}_{ii} \mathbf{h}_{\mathrm{p}} = \frac{\phi_{x_1 x_1} \gamma_{i,v}}{\gamma_{x,v}} (1 - \rho)^2 \kappa. \qquad (30)$$

The output SIR is then given by

$$\mathrm{SIR_o}(\mathbf{h}_{\mathrm{p}}) = \frac{\gamma_{x,v}}{\gamma_{i,v}} \cdot \frac{1}{(1 - \rho)^2 \kappa}. \qquad (31)$$

Finally, it is still important to evaluate the overall output SINR

$$\mathrm{SINR_o}(\mathbf{h}_{\mathrm{p}}) = \frac{\gamma_{x,v}(1 - \kappa)}{\wp(\rho)} \qquad (32)$$

with

$$\wp(\rho) = \kappa \left[1 + \gamma_{i,v}(1 - \kappa) \right] \rho^2$$
$$- 2 \gamma_{i,v} \kappa (1 - \kappa) \rho + (1 - \kappa)(1 + \gamma_{i,v} \kappa). \qquad (33)$$

The polynomial $\wp(\rho)$ is convex and strictly positive for $0 \le \rho \le 1$. Indeed, we can verify that its discriminant is given by $\Delta = -(1 + \gamma_{i,v})(1 - \kappa)\kappa \le 0$. $\wp(\rho)$ reaches its minimum at

$$\rho_1 = \frac{\gamma_{i,v}(1 - \kappa)}{1 + \gamma_{i,v}(1 - \kappa)}.$$

This particular value corresponds exactly to the MVDR that achieves the maximum SINR. The performance measures of the MVDR, LCMV, and matched filters are simply obtained from (28)–(32) by replacing ρ by ρ_1, 1, and 0, respectively. Specifically, we have

$$\mathrm{SNR_o}(\mathbf{h}_{\mathrm{MVDR}}) = \frac{\gamma_{x,v}}{1 + \frac{\gamma_{i,v}^2 \kappa (1 - \kappa)}{[1 + \gamma_{i,v}(1 - \kappa)]^2}} \qquad (34)$$

$$\mathrm{SIR_o}(\mathbf{h}_{\mathrm{MVDR}}) = \frac{\gamma_{x,v}}{\gamma_{i,v}} \cdot \frac{[1 + \gamma_{i,v}(1 - \kappa)]^2}{\kappa} \qquad (35)$$

$$\mathrm{SNR_o}(\mathbf{h}_{\mathrm{LCMV}}) = \gamma_{x,v}(1 - \kappa) \qquad (36)$$

$$\mathrm{SIR_o}(\mathbf{h}_{\mathrm{LCMV}}) = + \infty \qquad (37)$$

$$\mathrm{SNR_o}(\mathbf{h}_{\mathrm{MATCH}}) = \gamma_{x,v} \qquad (38)$$

and

$$\mathrm{SIR_o}(\mathbf{h}_{\mathrm{MATCH}}) = \frac{\gamma_{x,v}}{\gamma_{i,v} \kappa}. \qquad (39)$$

By observing expressions (29)–(39), we draw out two important remarks.

Remark 1: by increasing ρ, the parameterized filter is more focussed on interference reduction. The extreme case $\rho = 1$ corresponds to the LCMV which totally removes the interference, while the other extreme $\rho = 0$ ignores the interference and uniquely focusses on ambient noise reduction. The third extreme case corresponds to the MVDR which attempts to minimize the overall interference-plus-noise. Actually, we can easily prove by using (28) and (30) that $\mathrm{SNR_o}(\mathbf{h}_{\mathrm{p}})$ and $\mathrm{SIR_o}(\mathbf{h}_{\mathrm{p}})$ have opposite variations when ρ is varied. Indeed, $\mathrm{SIR_o}(\mathbf{h}_{\mathrm{p}})$ [respectively, $\mathrm{SNR_o}(\mathbf{h}_{\mathrm{p}})$] increases (respectively, decreases) with respect to ρ. For the three particular beamformers above, we have $\mathrm{SNR_o}(\mathbf{h}_{\mathrm{MATCH}}) \ge \mathrm{SNR_o}(\mathbf{h}_{\mathrm{MVDR}}) \ge \mathrm{SNR_o}(\mathbf{h}_{\mathrm{LCMV}})$ and $\mathrm{SIR_o}(\mathbf{h}_{\mathrm{MATCH}}) \le \mathrm{SIR_o}(\mathbf{h}_{\mathrm{MVDR}}) \le \mathrm{SIR_o}(\mathbf{h}_{\mathrm{LCMV}})$.

Remark 2: the collinearity factor κ plays a fundamental role in the performance of these filters. Indeed, for a given $\rho \ne 1$, increasing κ (by physically placing the noise source near the desired speech in the case of a white noise) leads to smaller output SNR and output SIR. The problem becomes quite complicated if we consider a reverberant enclosure where the existence of some frequencies for which κ has large values is more likely to be encountered than in anechoic environments for given spatial locations of the interference and the target signal. In such frequencies, the ambient noise can be amplified depending on the choice of ρ. For the LCMV, the output interference is always set to 0 at the price of a decreased output SNR that can reach very small values if $\kappa \to 1$.

C. Particular Case: Spatially White Noise

In this case, we have $\mathbf{\Phi}_{vv} = \sigma^2 \mathbf{I}$, $\gamma_{x,v} = \mathrm{SNR} \|\tilde{\mathbf{g}}\|^2$, $\gamma_{i,v} = \mathrm{INR} \|\tilde{\mathbf{d}}\|^2$, and $\kappa = \left| \tilde{\mathbf{g}}^{H} \tilde{\mathbf{d}} \right|^2 / \|\tilde{\mathbf{d}}\|^2 \|\tilde{\mathbf{g}}\|^2$. If we further assume that the
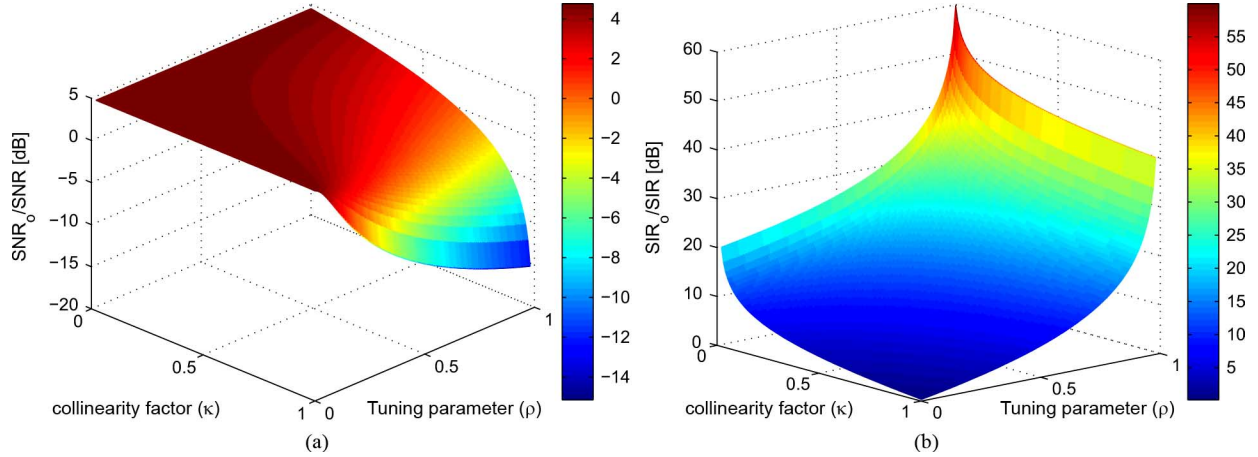
Fig. 1.   Theoretical effects the tuning parameter ρ and the collinearity factor κ on the performance of the parameterized filter (a) SNR gain (b) SIR gain.

environment only has as delay effect (plane-wave propagation model [8]), we obtain $\|\tilde{\mathbf{g}}\|^2 = \|\tilde{\mathbf{d}}\|^2 = M$ and

$$\mathrm{SNR_o}\,(\mathbf{h}_{\mathrm{p}}) = M\,\mathrm{SNR}\,\frac{1-\kappa}{1-(1-\rho^2)\,\kappa} \qquad (40)$$

$$\mathrm{SIR_o}\,(\mathbf{h}_{\mathrm{p}}) = \frac{\mathrm{SIR}}{\kappa\,(1-\rho)^2}. \qquad (41)$$

In particular, (34) to (39) become

$$\mathrm{SNR_o}\,(\mathbf{h}_{\mathrm{MVDR}}) = \frac{M\,\mathrm{SNR}}{1 + \frac{(M\,\mathrm{INR})^2\kappa(1-\kappa)}{[1+M\,\mathrm{INR}(1-\kappa)]^2}} \qquad (42)$$

$$\mathrm{SIR_o}\,(\mathbf{h}_{\mathrm{MVDR}}) = \mathrm{SIR}\,\frac{[1+M\,\mathrm{INR}\,(1-\kappa)]^2}{\kappa} \qquad (43)$$

$$\mathrm{SNR_o}\,(\mathbf{h}_{\mathrm{LCMV}}) = M\,(1-\kappa)\,\mathrm{SNR} \qquad (44)$$

$$\mathrm{SIR_o}\,(\mathbf{h}_{\mathrm{LCMV}}) = +\infty \qquad (45)$$

$$\mathrm{SNR_o}\,(\mathbf{h}_{\mathrm{MATCH}}) = M\,\mathrm{SNR} \qquad (46)$$

and

$$\mathrm{SIR_o}\,(\mathbf{h}_{\mathrm{MATCH}}) = \frac{\mathrm{SIR}}{\kappa}. \qquad (47)$$

The SNR gain achieved by $\mathbf{h}_{\mathrm{p}}$ depends on the tuning parameter, the number of microphones, and the collinearity factor.[2] On the other hand, its SIR gain depends on the collinearity factor and the tuning parameter only. For illustration purposes, we plot the theoretical expressions of SNR and SIR gains [i.e., $\mathrm{SNR_o}\,(\mathbf{h}_{\mathrm{p}})/\mathrm{SNR}$ and $\mathrm{SIR_o}\,(\mathbf{h}_{\mathrm{p}})/\mathrm{SIR}$ obtained from (40) and (41), respectively] and show the effects of κ and ρ in Fig. 1 for $M = 3$. There, we observe the tradeoff between the interference rejection and noise reduction. Indeed, by increasing the tuning parameter towards 1, $\mathbf{h}_{\mathrm{p}}$ is more focussed on interference rejection at the price of a decreased output SNR. This behavior is more remarkable for a sufficiently high collinearity factor. When the latter is sufficiently low, the degradation of the output SNR is less noticeable. From this figure, we also deduce the effect of the collinearity factor on the extreme cases of the LCMV and matched beamformers. We have previously established that the LCMV achieves the poorest output SNR. Precisely, the SNR gain of the LCMV (compared to the matched filter) is reduced by the geometrical factor $1 - \kappa$, thereby meaning that the

[2]Note that κ depends not only on the number of microphones, but also on the array geometry, and the spatial separation between the desired source and the interference.

larger is the collinearity between the propagation vector of the interference and the desired source, the lower is the output SNR. Hence, total removal of the interference may come at the price of an amplified ambient noise [notice the negative SNR gains in Fig. 1(a)]. This happens when $\kappa \geq 1 - 1/M$. Since $\kappa \leq 1$, we can deduce that the larger is M, the larger is $1 - 1/M$, and the lower are the chances to have an amplified output ambient noise (since κ itself depends on M). The matched filter is able to achieve the interference reduction for non-collinear interference and source steering vectors (this is not necessarily the case for a reverberant environment or a general type of noise). However, this gain may be negligible when the collinearity factor is sufficiently high. It seems less obvious to deduce the effect of both parameters on the MVDR beamformer from Fig. 1 since $\rho_{\mathrm{MVDR}} = \rho_1$ depends on INR and κ. Therefore, we provide Fig. 2 which is obtained from (42) and (43). We notice that the MVDR attempts to balance both effects: noise reduction and interference rejection especially when the collinearity factor takes relatively large values. Indeed, when the input INR is large, this filter is more focussed on the rejection of the interference. This comes at the price of a decreased output SNR. For instance, we see that for very large input INR (e.g., 20 dB or more) the SNR gain takes negative values which means that the ambient noise is amplified. At the same values we notice that the SIR gain becomes more important. When the collinearity factor is sufficiently small, the MVDR can achieve high SNR and SIR gains simultaneously.

V. NUMERICAL EXAMPLES

In this section, we aim at numerically corroborating our theoretical findings. To this end, we consider two types of unknown noise: spatially white and diffuse (see definition in Section V-C). The latter is typically encountered in highly reverberant enclosures [19]. For the sake of simplicity, we consider a planar configuration where the target source, the interference, and the microphones are located on a single plane. In this setup, we consider a uniform linear array (ULA) of microphones with δ being the inter-microphone spacing. δ will be chosen depending on the simulated scenario. The source and the interference have azimuthal angles $\theta_s = 120°$ and $\theta_i = \theta_s - \Delta\theta$ which are measured counter-clockwise from the array axis. $\Delta\theta$ will be chosen depending on the examples investigated below. Also, we found as expected that the LCMV achieves a much larger output SIR (theoretically infinite) than the MVDR and matched filters in all cases. For the sake of clarity, we will avoid showing this output SIR and mention that it is infinite on Figs. 3(b), 7, and 10.
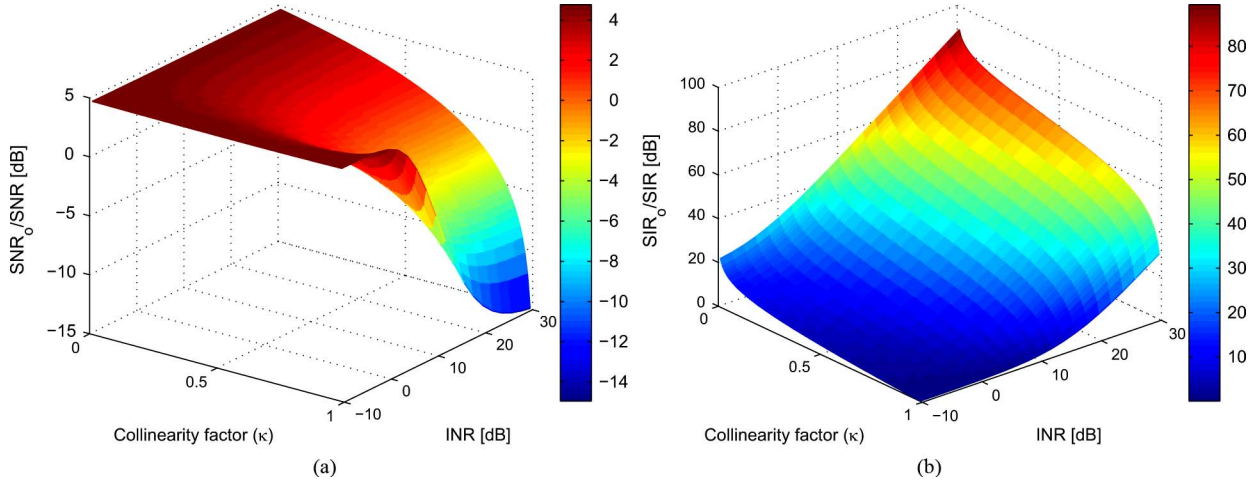
Fig. 2. Theoretical effects the input INR an the collinearity factor κ on the performance of the MVDR filter (a) SNR gain (b) SIR gain.
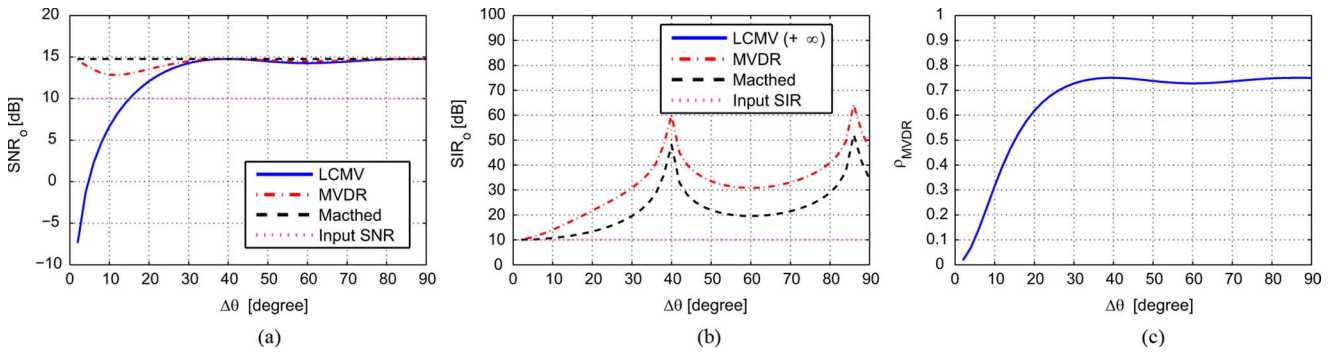

Fig. 3. Effect of the angular separation $\Delta\theta$ between the interference and the target source on the performance of the MVDR, LCMV, and matched filters; spatially white noise and anechoic room (a) Output SNR versus $\Delta\theta$ (b) Output SIR versus $\Delta\theta$ (c) ρ_{MVDR} versus $\Delta\theta$.

To have a clear understanding of the investigated problem, we chose to study two scenarios. In the first one, we assume that the target source and the interference are located in the far field with no reverberation. Subsequently, the corresponding steering vectors are well known to be $\mathbf{g}(j\omega) = \begin{bmatrix} 1 \ e^{j\omega\delta/c\cos(\theta_s)} \ \cdots \ e^{j\omega(M-1)\delta/c\cos(\theta_s)} \end{bmatrix}^T$ and $\mathbf{d}(j\omega) = \begin{bmatrix} 1 \ e^{j\omega\delta/c\cos(\theta_i)} \ \cdots \ e^{j\omega(M-1)\delta/c\cos(\theta_i)} \end{bmatrix}^T$, respectively, at a given frequency ω. $c = 343 \ \mathrm{ms}^{-1}$ is the speed of sound. Then, we form the PSD matrices as $\boldsymbol{\Phi}_{xx} = \phi_{ss}\mathbf{g}\mathbf{g}^H$, and $\boldsymbol{\Phi}_{ii} = \phi_{ii}\mathbf{d}\mathbf{d}^H$. In the second scenario, we consider a reverberant enclosure which is simulated using the modified version of Allen and Berkley's image method [10], [11]. The simulated room has dimensions 3.048-by-4.572 by-3.81 m³. The microphone elements are placed on the axis $(y_0 = 1.016, z_0 = 1.016)$ m with the center of the microphone being at $(x_0 = 1.524 \ \mathrm{m}, y_0, z_0)$ and the nth one at $(x_0 - M - 2n + 1/2\delta, y_0, z_0)$ with $n = 1, \ldots, M$. The interference and the source are located at a distance of 2.50 m away from the center of the microphone array. The walls, ceiling, and floor reflection coefficients are set to achieve a reverberation decay time $T_{60} = 200$ ms measured using the backward integration method (see [2, Ch. 2] for more details).

A. Spatially White Noise Plus Interference in an Anechoic Environment

This case corresponds to the plane-wave propagation model with spatially white noise that was considered in [8] to study the beampattern of the MVDR. Here, we would rather analyze the SNR and SIR at the output of this beamformer in addition to the LCMV and matched filters. Evaluating both objective measures is more meaningful than the visual inspection of the beampatterns in speech enhancement applications. We investigate the effect of $\Delta\theta$ on the performance of the MVDR, LCMV, and matched filters. We choose $\mathrm{SIR} = 10$ dB and $\mathrm{SNR} = 10$ dB. The performance of the filters is assessed at a frequency $f = 1000$ Hz and the inter-microphones spacing is set such that $\delta = c/2f$ to prevent spatial aliasing. We choose the number of microphones as $M = 3$. Fig. 3(a) and (b) depicts the effect of $\Delta\theta$ on the SIR and SNR at the output of the three beamformers. It is clearly seen that decreasing $\Delta\theta$ decreases the output SNR of the LCMV. We particularly see that the output SNR is even lower than the input SNR for $\Delta\theta < 15°$. The output SNR of the MVDR and matched filters are almost unaffected while very low output SIR values are obtained for small $\Delta\theta$. Moreover, we observe the beampatterns as in [8] to justify the variations of the SNR and SIR for not only the MVDR but also the LCMV and matched filters. In Fig. 4, the beampatterns of the three beamformers for three values of $\Delta\theta$: 60°, 20°, and 10° are depicted. When $\Delta\theta$ decreases, two major behaviors of the MVDR and LCMV emerge: displacement of the main beam away from the source location and appearance of sidelobes. To explain these behaviors, recall that in the formulation of the optimization problems leading to the LCMV and MVDR, the array response towards the source direction is forced to the unity gain. This constraint is satisfied in the provided results (the maximum of both beampatterns correspond to values larger than one and the results presented in Fig. 4 are normalized with respect to the largest value). Physically, as the interference moves towards the target source, it becomes harder for the LCMV to satisfy two contradictory constraints: switching the gain from zero to one. This fact results
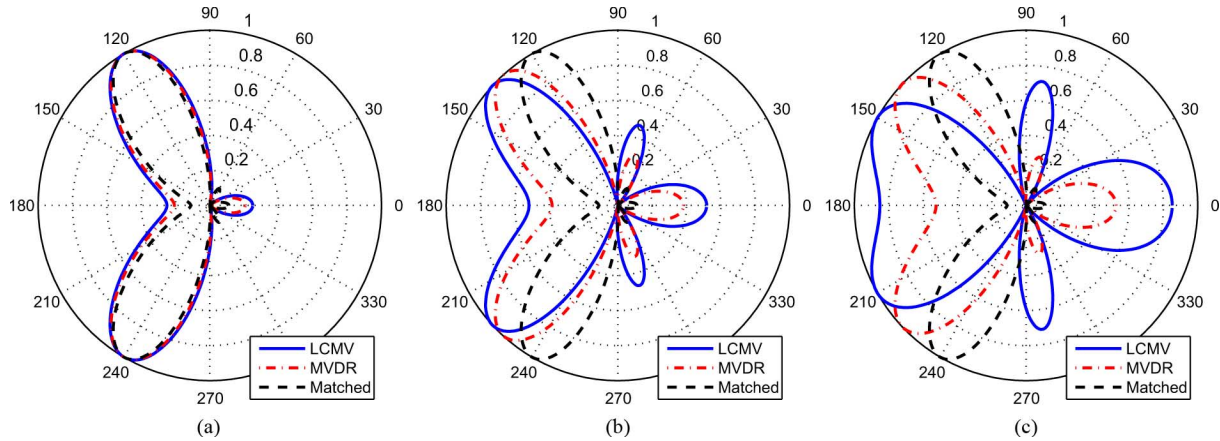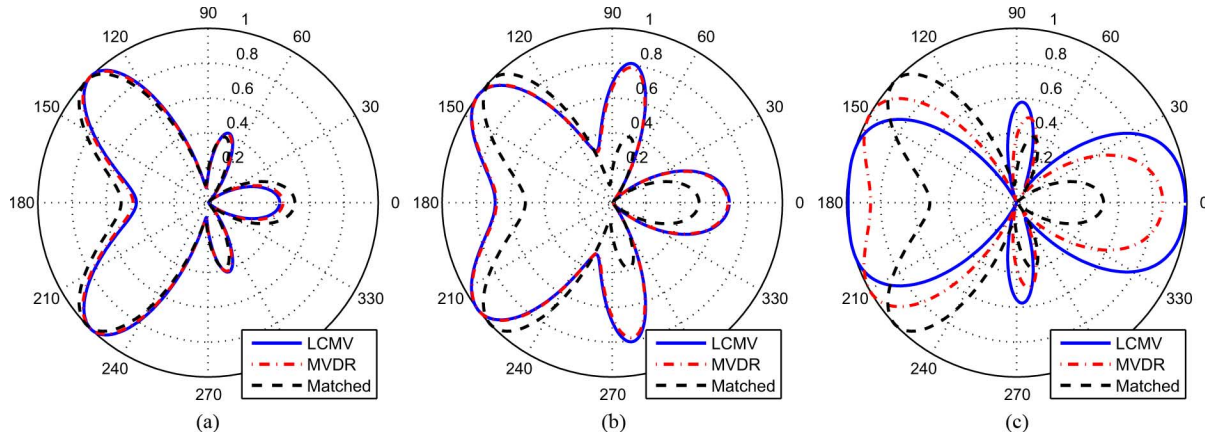
Fig. 4. Beampatterns of the MDR, LCMV, and matched filters; the source is at $120°$ and the interference is at $120° - \Delta\theta$, spatially white noise and anechoic room (a) $\Delta\theta = 60°$ (b) $\Delta\theta = 20°$ (c) $\Delta\theta = 10°$.

Fig. 5. Beampatterns of the MDR, LCMV, and matched filters; the source is at $120°$ and the interference is at $120° - \Delta\theta$, spatially white noise and reverberant room (a) $\Delta\theta = 60°$ (b) $\Delta\theta = 20°$ (c) $\Delta\theta = 10°$.

in instabilities that translate into the appearance of sidelobes and displacement of the maximum far from the interference. These sidelobes lead the beamformers to capture the white noise which spans the whole space. This physical interpretation is corroborated by our theoretical study above and the results provided in Fig. 3. Finally, it is obvious that when $\Delta\theta$ increases, the three filters perform relatively well, especially in terms of noise removal. In Fig. 3(c), we see that $\rho_{\mathrm{MVDR}} = \rho_1$, defined in (20), tends to take large values when $\Delta\theta$ increases, until it reaches an upper bound which is lower than one due to the coexistence of both interference and ambient noise. In terms of interference removal, the LCMV obviously outperforms both other beamformers. This suggests that the LCMV could be a very good candidate for interference removal when the latter is placed far from the target source. However, one has to be very careful when using this filter because of the potential instabilities that it exhibits when this spatial separation is low, as discussed above.

B. Spatially White Noise Plus Interference in a Reverberant Environment

The three beampatterns depicted in Fig. 5 undoubtedly illustrate the detrimental effect of the reverberation when compared to those of Fig. 4. The sidelobes are amplified, as compared to the anechoic case, even with $\Delta\theta = 60°$, but become larger when $\Delta\theta$ is decreased. Similarly, we see that placing the interference near the source dramatically deteriorates the beampatterns of the MVDR and LCMV. For

example, notice that when $\Delta\theta = 10°$ the LCMV and MVDR almost steer a "relative" zero toward the source direction of arrival (located at $120°$). The matched beamformer exhibits the same beampattern since it is independent of $\Delta\theta$. Since the noise is white, moving the interference near the desired signal increases the similarity between the propagation vectors. Indeed, the collinearity factor defined in (9) increases in the case of a white noise when the similarity between the transfer function vectors $\tilde{\mathbf{d}}$ and $\tilde{\mathbf{g}}$ is increased, which is physically more likely to happen when the source and interference are spatially close. Figs. 6 and 7 show the effect of $\Delta\theta$ on the output SNR and output SIR, respectively. This effect is actually frequency dependent as we can see a wide dynamic range of both performance measures for the investigated frequency band. However, we can notice that the infinite gain in SIR achieved by the LCMV may come at the price of very low output SNR as compared to the other two filters, especially in the low frequency range (lower than 500 Hz). When we compare Figs. 6(a)–6(c), we notice that when the interference is spatially close to the target source, a remarkable performance degradation is observed in terms of output SNR especially for the LCMV filter, and in terms of output SIR especially for the MVDR and matched filters.

C. Spatially Diffuse Noise Plus Interference in a Reverberant Environment

The cross-coherence between the spatially diffuse noise signals observed by a pair of microphones (k, l) is $\Gamma_{v_k v_l}(\omega) =$
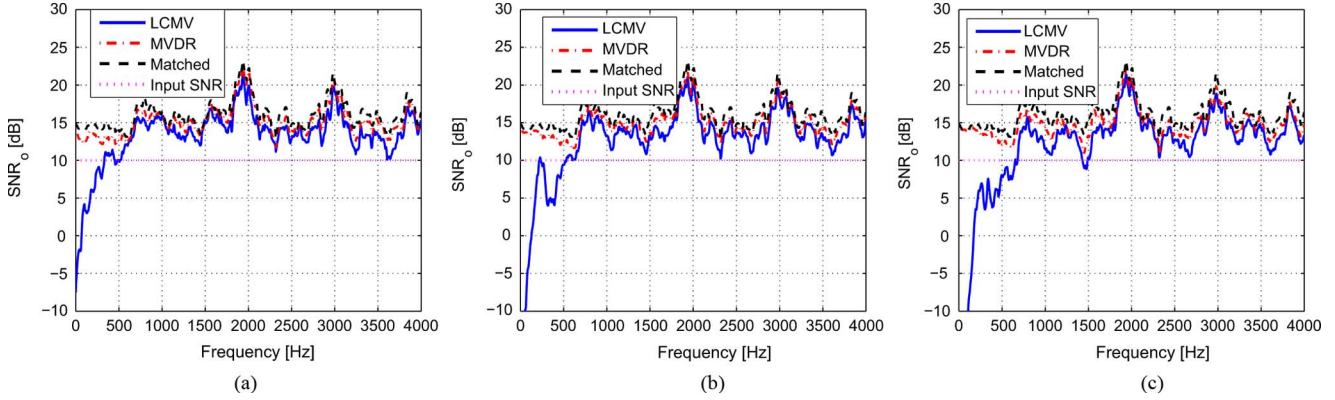
Fig. 6.   SNR at the output of the LCMV, MVDR, and matched filters; white noise and reverberant room (a) $\Delta\theta = 60°$ (b) $\Delta\theta = 20°$ (c) $\Delta\theta = 10°$.
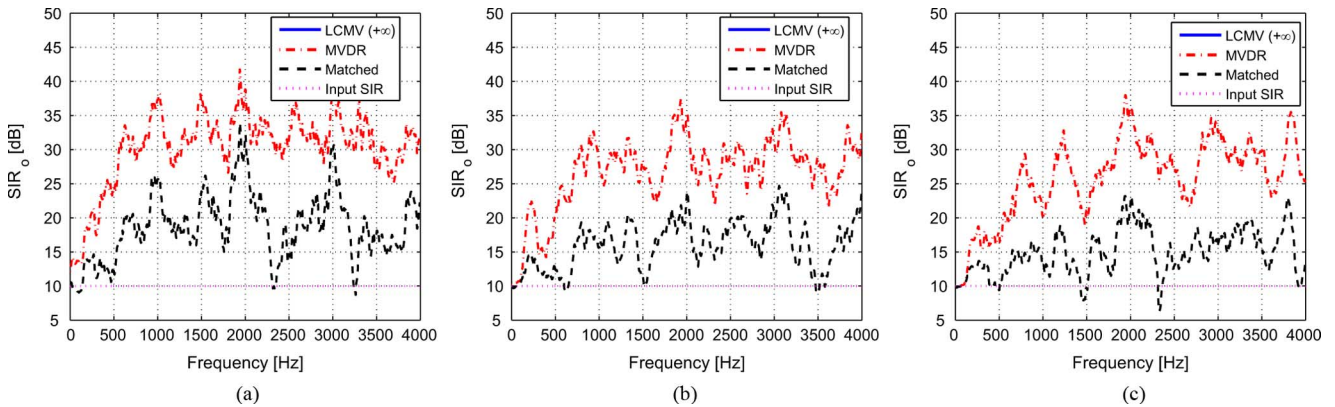

Fig. 7.   SIR at the output of the LCMV, MVDR, and matched filters; white noise and reverberant room (a) $\Delta\theta = 60°$ (b) $\Delta\theta = 20°$ (c) $\Delta\theta = 10°$.
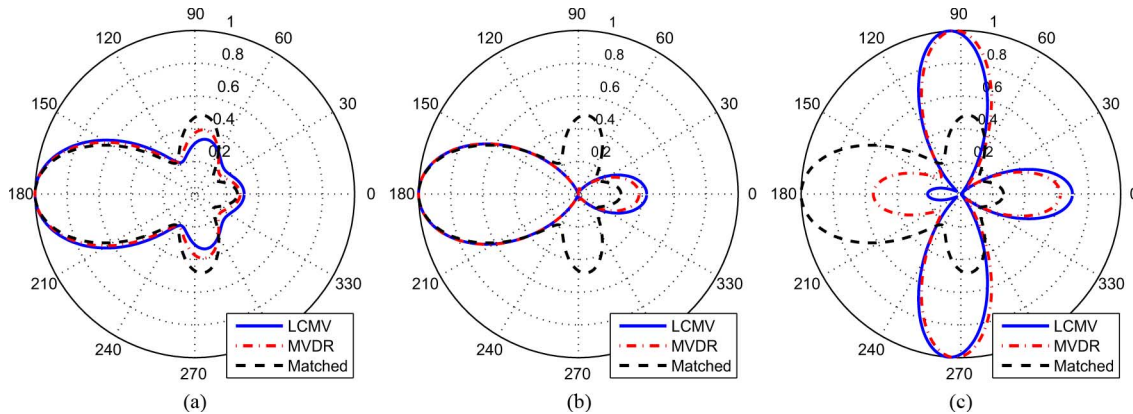

Fig. 8.   Beampatterns of the MDR, LCMV, and matched filters; the source is at $120°$ and the interference is at $120° - \Delta\theta$, spatially diffuse noise and reverberant room (a) $\Delta\theta = 60°$ (b) $\Delta\theta = 20°$ (c) $\Delta\theta = 10°$.

$\sin(\omega\delta_{kl}/c)/\omega\delta_{kl}/c$, at a given frequency ω, where δ_{kl} is the distance between both sensors [17], [19]. In our case, $\delta_{kl} = (k - l)\delta$. Thus, choosing $\delta = c/2f$ results in a spatially white noise. To avoid this redundancy (see previous section about white noise and reverberant enclosure), we choose $\delta = c/5f$.

The beampatterns in Fig. 8 show the deleterious effect of the diffuse noise in addition to the reverberation when compared to Figs. 4 and 5. Thus, the classical plane-wave propagation model-based MVDR [8] may fail to reconstruct the target signal in this scenario since the main lobes of the beampatterns are not even pointed toward the vicinity of the target source (located at $120°$). In Figs. 9 and 10, it is observed that the diffuse noise has a quite different effect on the output SIR and output SNR for the three filters, as compared to the white noise case. For instance, we see that a better behavior of the LCMV in terms of output SNR is obtained for the low frequency range. When the interference is moved towards the desired source, the LCMV exhibits a remarkable output SNR degradation as seen in Fig. 9 while the MVDR and matched beamformers lead to significant losses in terms of ouput SIR as shown in Fig. 10. These behaviors are explained by the increased similarity of propagation vectors of the interference and the desired source in the transform domain defined by the diffuse noise PSD matrix as explained in Section III.
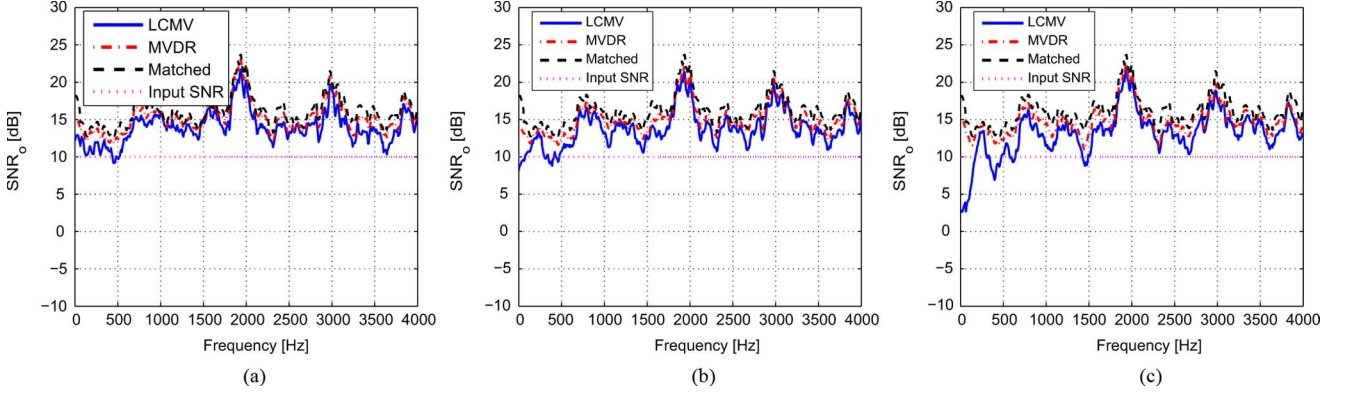
Fig. 9.   SNR at the output of the LCMV, MVDR, and matched filters; white noise and reverberant room (a) $\Delta\theta = 60°$ (b) $\Delta\theta = 20°$ (c) $\Delta\theta = 10°$.
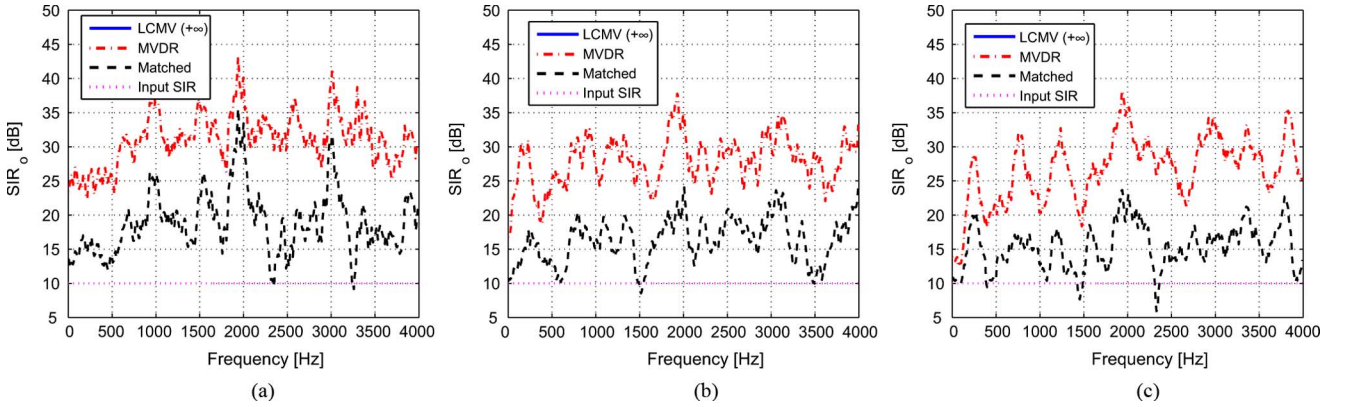

Fig. 10.   SIR at the output of the LCMV, MVDR, and matched filters; spatially diffuse noise and reverberant room (a) $\Delta\theta = 60°$ (b) $\Delta\theta = 20°$ (c) $\Delta\theta = 10°$.

VI. CONCLUSION

In this contribution, we provided new insights into the MVDR and LCMV beamformers in the context of noise reduction. We considered the case where both interference and ambient noise coexist with the target speech signal and demonstrated a new relationship between both filters in which the MVDR is shown to be a linear combination of the LCMV and a matched filter (MVDR solution when only ambient noise overlaps with the target signal). Both components are optimally weighted such that maximum interference-plus-noise attenuation is achieved. We also proposed a generic expression of a parameterized distortionless noise reduction filter of which the MVDR, LCMV, and matched filters are particular cases. We analyzed the noise and interference reduction capabilities of this generic filter with a special focus on the MVDR, LCMV, and matched filters. Specifically, we developed new closed-form expressions for the SNR and SIR at the output of all the investigated filters. These expressions theoretically demonstrate the tradeoff between noise and interference reduction. Indeed, total removal of the interference (by the LCMV) may result in the magnification of the ambient noise. Similarly, totally focussing on the ambient noise reduction (by the matched filter) may result in very poor output SIR. Our findings were finally corroborated by numerical evaluations in simulated acoustic environments. Nevertheless, the proposed analysis is general and remains valid for similar situations where the channel is modeled by generalized transfer functions and the additive noise has arbitrary PSD matrix.

APPENDIX I
PROOF OF THE NEW RELATIONSHIP BETWEEN THE MVDR AND THE LCMV

To prove this new relationship, we need to express (14) and (18) differently as explained below. First, according to the matrix inversion lemma, we have

$$(\boldsymbol{\Phi}_{ii} + \boldsymbol{\Phi}_{vv})^{-1} = \boldsymbol{\Phi}_{vv}^{-1} - \frac{\boldsymbol{\Phi}_{vv}^{-1}\boldsymbol{\Phi}_{ii}\boldsymbol{\Phi}_{vv}^{-1}}{1 + \gamma_{i,v}} \qquad (48)$$

where $\gamma_{i,v}$ is defined in (6). Plugging (5), (11), and (48) into (14), we obtain an equivalent expression for the MVDR that still depends on the interference, noise, and target signal statistics only

$$\mathbf{h}_{\text{MVDR}} = \frac{(1 + \gamma_{i,v})\,\mathbf{I} - \boldsymbol{\Phi}_{vv}^{-1}\boldsymbol{\Phi}_{ii}}{\gamma + \gamma_{x,v}}\boldsymbol{\Phi}_{vv}^{-1}\boldsymbol{\Phi}_{xx}\mathbf{u}_1 \qquad (49)$$

where $\mathbf{I}$ is the $M \times M$ identity matrix.

To find the alternative expression of the LCMV, we start by replacing $\mathbf{C}$ by its expression in (18) and first compute $\mathbf{C}^H\boldsymbol{\Phi}_{vv}^{-1}\mathbf{C}$ which is a 2×2 matrix whose inverse is given by

$$\left(\mathbf{C}^H \boldsymbol{\Phi}_{vv}^{-1}\mathbf{C}\right)^{-1} = \frac{\phi_{ss}\phi_{ii}}{\gamma}\begin{bmatrix} \mathbf{d}^H\boldsymbol{\Phi}_{vv}^{-1}\mathbf{d} & -\mathbf{g}^H\boldsymbol{\Phi}_{vv}^{-1}\mathbf{d} \\ -\mathbf{d}^H\boldsymbol{\Phi}_{vv}^{-1}\mathbf{g} & \mathbf{g}^H\boldsymbol{\Phi}_{vv}^{-1}\mathbf{g} \end{bmatrix}. \qquad (50)$$

Plugging (50) into (18) and using the results $G_1^* = \mathbf{g}^H\mathbf{u}_1$ and $\mathbf{g}^H\boldsymbol{\Phi}_{vv}^{-1}\mathbf{g} = \text{tr}\left[\boldsymbol{\Phi}_{vv}^{-1}\boldsymbol{\Phi}_{xx}\right]/\phi_{ss}$, we obtain

$$\mathbf{h}_{\text{LCMV}} = \frac{\gamma_{i,v}\mathbf{I} - \boldsymbol{\Phi}_{vv}^{-1}\boldsymbol{\Phi}_{ii}}{\gamma}\boldsymbol{\Phi}_{vv}^{-1}\boldsymbol{\Phi}_{xx}\mathbf{u}_1. \qquad (51)$$

$$\mathbf{h}_{\mathrm{LCMV}}^{H}\boldsymbol{\Phi}_{vv}\mathbf{h}_{\mathrm{LCMV}} = \frac{\phi_{x_1 x_1}}{\gamma^2}\left\{\gamma_{i,v}^2\,\mathrm{tr}\left[\boldsymbol{\Phi}_{vv}^{-1}\boldsymbol{\Phi}_{xx}\right] + \mathrm{tr}\left[\boldsymbol{\Phi}_{vv}^{-1}\boldsymbol{\Phi}_{ii}\boldsymbol{\Phi}_{vv}^{-1}\boldsymbol{\Phi}_{ii}\boldsymbol{\Phi}_{vv}^{-1}\boldsymbol{\Phi}_{xx}\right] - 2\gamma_{i,v}\,\mathrm{tr}\left[\boldsymbol{\Phi}_{vv}^{-1}\boldsymbol{\Phi}_{ii}\boldsymbol{\Phi}_{vv}^{-1}\boldsymbol{\Phi}_{xx}\right]\right\}$$

$$= \frac{\phi_{x_1 x_1}}{\gamma^2}\left\{\gamma_{i,v}^2\,\gamma_{x,v} + \gamma_{i,v}^2\,\gamma_{x,v}\,\mathrm{tr}\left[\mathbf{c}_i\mathbf{l}_i^T\mathbf{c}_i\mathbf{l}_i^T\mathbf{c}_x\mathbf{l}_x^T\right] - 2\gamma_{i,v}^2\,\gamma_{x,v}\mathbf{l}_i^T\mathbf{c}_x\mathbf{l}_x^T\mathbf{c}_i\right\}. \tag{54}$$

Now, using (49) and (51), we conclude that we have the relationship in (19) and (20).

APPENDIX II
PROOF OF (28) AND (30)

Using (26) we can easily compute

$$\mathbf{h}_{\mathrm{p}}^{H}\boldsymbol{\Phi}_{vv}\mathbf{h}_{\mathrm{p}} = \rho^2\mathbf{h}_{\mathrm{LCMV}}^{H}\boldsymbol{\Phi}_{vv}\mathbf{h}_{\mathrm{LCMV}}$$
$$+ (1-\rho)^2\,\mathbf{h}_{\mathrm{MATCH}}^{H}\boldsymbol{\Phi}_{vv}\mathbf{h}_{\mathrm{MATCH}}$$
$$+ \rho\,(1-\rho)\,\mathbf{h}_{\mathrm{MATCH}}^{H}\boldsymbol{\Phi}_{vv}\mathbf{h}_{\mathrm{LCMV}}$$
$$+ \rho\,(1-\rho)\,\mathbf{h}_{\mathrm{LCMV}}^{H}\boldsymbol{\Phi}_{vv}\mathbf{h}_{\mathrm{MATCH}}. \tag{52}$$

Now, we compute each of the above terms on the right-hand side

$$\mathbf{h}_{\mathrm{LCMV}}^{H}\boldsymbol{\Phi}_{vv}\mathbf{h}_{\mathrm{LCMV}}$$
$$= \frac{1}{\gamma^2}\left(\gamma_{i,v}^2\mathbf{u}_1^T\boldsymbol{\Phi}_{xx}\boldsymbol{\Phi}_{vv}^{-1}\boldsymbol{\Phi}_{xx}\mathbf{u}_1\right.$$
$$+ \mathbf{u}_1^T\boldsymbol{\Phi}_{xx}\boldsymbol{\Phi}_{vv}^{-1}\boldsymbol{\Phi}_{ii}\boldsymbol{\Phi}_{vv}^{-1}\boldsymbol{\Phi}_{ii}\boldsymbol{\Phi}_{vv}^{-1}\boldsymbol{\Phi}_{xx}\mathbf{u}_1$$
$$\left. - 2\gamma_{i,v}\mathbf{u}_1^T\boldsymbol{\Phi}_{xx}\boldsymbol{\Phi}_{vv}^{-1}\boldsymbol{\Phi}_{ii}\boldsymbol{\Phi}_{vv}^{-1}\boldsymbol{\Phi}_{xx}\mathbf{u}_1\right). \tag{53}$$

Note that for a given matrix $\mathbf{M}$, we have $\mathbf{u}_1^T\boldsymbol{\Phi}_{xx}\mathbf{M}\boldsymbol{\Phi}_{xx}\mathbf{u}_1 = \phi_{x_1 x_1}\mathrm{tr}\left[\mathbf{M}\boldsymbol{\Phi}_{xx}\right]$. Then, (53) becomes (54), shown at the top of the page. According to the definitions of $\mathbf{l}_x^T$, $\mathbf{c}_x$, $\mathbf{l}_i^T$, and $\mathbf{c}_i$ in Property 1, we have $\mathbf{l}_x^T\mathbf{c}_x = \mathbf{l}_i^T\mathbf{c}_i = 1$. Thus,

$$\mathbf{h}_{\mathrm{LCMV}}^{H}\boldsymbol{\Phi}_{vv}\mathbf{h}_{\mathrm{LCMV}} = \frac{\phi_{x_1 x_1}}{\gamma_{x,v}(1-\kappa)}. \tag{55}$$

Also, we easily compute

$$\mathbf{h}_{\mathrm{MATCH}}^{H}\boldsymbol{\Phi}_{vv}\mathbf{h}_{\mathrm{MATCH}} = \frac{\phi_{x_1 x_1}}{\gamma_{x,v}}. \tag{56}$$

Using (15) and (51), we compute

$$\mathbf{h}_{\mathrm{MATCH}}^{H}\boldsymbol{\Phi}_{vv}\mathbf{h}_{\mathrm{LCMV}}$$
$$= \frac{1}{\gamma_{x,v}\gamma}\left(\gamma_{i,v}\mathbf{u}_1^T\boldsymbol{\Phi}_{xx}\boldsymbol{\Phi}_{vv}^{-1}\boldsymbol{\Phi}_{xx}\mathbf{u}_1\right.$$
$$\left. -\mathbf{u}_1^T\boldsymbol{\Phi}_{xx}\boldsymbol{\Phi}_{vv}^{-1}\boldsymbol{\Phi}_{ii}\boldsymbol{\Phi}_{vv}^{-1}\boldsymbol{\Phi}_{xx}\mathbf{u}_1\right)$$
$$= \frac{\phi_{x_1 x_1}}{\gamma_{x,v}\gamma}\left(\gamma_{i,v}\gamma_{x,v} - \gamma_{i,v}\gamma_{x,v}\kappa\right)$$
$$= \frac{\phi_{x_1 x_1}}{\gamma_{x,v}}. \tag{57}$$

Using (52), (55)–(57), we obtain (28).

To compute the residual interference power in (30), we know that $\mathbf{h}_{\mathrm{LCMV}}^{H}\boldsymbol{\Phi}_{ii}\mathbf{h}_{\mathrm{MATCH}} = 0$. Hence,

$$\mathbf{h}_{\mathrm{p}}^{H}\boldsymbol{\Phi}_{ii}\mathbf{h}_{\mathrm{p}} = (1-\rho)^2\mathbf{h}_{\mathrm{MATCH}}^{H}\boldsymbol{\Phi}_{ii}\mathbf{h}_{\mathrm{MATCH}}$$
$$= \frac{(1-\rho)^2\phi_{x_1 x_1}}{\gamma_{x,v}^2}\mathrm{tr}\left[\boldsymbol{\Phi}_{vv}^{-1}\boldsymbol{\Phi}_{ii}\boldsymbol{\Phi}_{vv}^{-1}\boldsymbol{\Phi}_{xx}\right]$$

$$= \frac{\phi_{x_1 x_1}\gamma_{i,v}}{\gamma_{x,v}}(1-\rho)^2\kappa. \tag{58}$$

This completes the proof. □

REFERENCES

[1] Y. Kaneda and J. Ohga, "Adaptive microphone-array system for noise reduction," *IEEE Trans. Acoust., Speech, Signal Process.*, vol. ASSP-34, pp. 1391–1400, Dec. 1986.

[2] Y. Huang, J. Benesty, and J. Chen, *Acoustic MIMO Signal Processing*. Berlin, Germany: Springer-Verlag, 2006.

[3] S. Gannot, D. Burshtein, and E. Weinstein, "Signal enhancement using beamforming and nonstationarity with applications to speech," *IEEE Trans. Signal Process.*, vol. 49, no. 8, pp. 1614–1626, Aug. 2001.

[4] G. Reuven, S. Gannot, and I. Cohen, "Dual source transfer-function generalized sidelobe canceller," *IEEE Trans. Audio, Speech, Lang. Process.*, vol. 16, pp. 711–726, May 2008.

[5] M. Souden, J. Benesty, and S. Affes, "New insights into non-causal multichannel linear filtering for noise reduction," in *Proc. IEEE ICASSP*, Taipei, Taiwan, Apr. 19–24, 2009, pp. 141–144.

[6] P. C. Loizou, *Speech Enhancement: Theory and Practice*. New York: CRC Press, 2007.

[7] J. Benesty, J. Chen, and Y. Huang, *Microphone Array Signal Processing*. Berlin, Germany: Springer-Verlag, 2008.

[8] H. L. Van Trees, *Dection, Estimation, and Modulation Theory Part IV: Optimum Array processing*. New York: Wiley, 2002.

[9] M. Wax and Y. Anu, "Performance analysis of the minimum variance beamformer," *IEEE Trans. Signal Process.*, vol. 44, no. 4, pp. 928–937, Apr. 1996.

[10] J. B. Allen and D. A. Berkley, "Image method for efficiently simulating small-room acoustics," *J. Acoust. Soc. Amer.*, vol. 65, pp. 943–950, Apr. 1979.

[11] P. Peterson, "Simulating the response of multiple microphones to a single acoustic source in a reverberant room," *J. Acoust. Soc. Amer.*, vol. 80, pp. 1527–152, Nov. 1986.

[12] J. Capon, "High-resolution frequency-wavenumber spectrum analysis," *Proc. IEEE*, vol. 57, pp. 1408–1418, Aug. 1969.

[13] O. Frost, "An algorithm for linearly constrained adaptive array processing," *Proc. IEEE*, vol. 60, pp. 926–934, 1972.

[14] S. Affes and Y. Grenier, "A signal subspace tracking algorithm for microphone array processing of speech," *IEEE Trans. Speech, Audio Process.*, vol. 5, pp. 425–437, Sep. 1997.

[15] L. Griffiths and C. W. Jim, "An alternative approach to linearly constrained adaptive beamforming," *IEEE Trans. Antennas Propagat.*, vol. AP-30, pp. 27–34, Jan. 1982.

[16] S. Markovich, S. Gannot, and I. Cohen, "Multichannel eigenspace beamforming in a reverberant noisy environment with multiple interfering speech signals," *IEEE Trans. Audio, Speech, Lang. Process.*, vol. 17, pp. 1071–108, Aug. 2009.

[17] J. Bitzer, K. Simmer, and K.-D. Kammeyer, "Theoretical noise reduction limits of the generalized sidelobecanceller (GSC) for speech enhancement," in *Proc. IEEE ICASSP*, 1999, pp. 2965–2968.

[18] B. R. Breed and J. Strauss, "A short proof of the equivalence of LCMV and GSC beamforming," *IEEE Signal Process. Lett.*, vol. 9, pp. 168–169, Jun. 2002.

[19] S. Gannot and I. Cohen, *Springer Handbook of Speech Processing*. Berlin, Germany: Springer-Verlag, 2007, ch. Adaptive Beamforming and Postfitering, pp. 945–978.

[20] P. Comon, "Independent component analysis, a new concept?," *Elsevier, Signal Process.*, vol. 36, pp. 287–314, Apr. 1994.